SOVIET PHYSICS USPEKHI VOLUME 13, NUMBER 6 MAY-JUNE, 1971

533.601.155/9

IONIZATION RELAXATION BEHIND STRONG SHOCK WAVES IN GASES

L. M. BIBERMAN, A. Kh. MNATSAKANYAN, and I. T. YAKUBOV

Institute for High Temperatures, USSR Academy of Sciences

Usp. Fiz. Nauk 102, 431—462 (November, 1970)

1. INTRODUCTION

THE passage of a strong shock wave (SW) is accompanied by a sharp change in the state of the gas. In the strong compression jump (within the SW front) at a distance of the order of the mean free path the energy of the directed motion is transformed into thermal energy; the advancing temperature of the gas increases sharply. The excitation of internal degrees of freedom occurs over considerably longer time intervals. As a result a rather extensive region is formed behind the SW in which the concentrations of particles, as well as their distribution over energy levels, relax to a final thermodynamic state of equilibrium.

In the case of weak SW in molecular gases the rate of establishment of equilibrium is determined by the rotational relaxation and by various chemical reactions (for instance, by the dissociation). With increasing velocities of the SW these processes occur more rapidly, and the ionization becomes the process that determines the extent of the nonequilibrium region. The final equilibrium state in this case is an atomic plasma. An appreciable portion of the energy of the incoming flux is dissipated in its production.

The following are tentative characteristics of the nonequilibrium region in this case: number of particles 10^{15}—10^{19} cm^{-3}, temperatures of the order of several eV, and relaxation times of 1—10^3 μsec. Ionization relaxation is thus a comparatively slow process realized by numerous sequential collisions. The theoretical task is to determine the temperature profiles and concentrations of the principal components, their distributions over excited states and, as a result of this, to calculate the relaxation times.

Relaxation phenomena behind SW were discussed in reviews* and monographs.[1-6] However, the problems of ionization relaxation could not be treated with sufficient completeness in these papers, inasmuch as the main results in this field have only been obtained in the last few years. These successes were due to intensive experimental investigations for large Mach numbers, as well as to progress in the theory of kinetics in low-temperature plasmas. In this review we have attempted to sum up the results of recent years in the field of ionization relaxation and draw attention to a series of still unsolved problems.

1.1. Fundamental Equations. Brief Contents of the Review

An important step in the study of the development of ionization behind a SW was the paper of Petschek and Byron[9] who investigated SW in argon experimentally and theoretically. They established that the relaxation occurs in two stages. A relatively slow generation of electrons occurs during the first stage. After the electron concentration reaches a given magnitude, the relaxation is completed by cumulative ionization by means of electron impact. Subsequent investigations of strong SW in atomic and molecular gases (predominantly in air) showed that the elementary processes giving rise to ionization during the first stage can be very diverse. The rate of cumulative ionization depends markedly on the energy of the electrons and is thus determined by the energy balance of the electron gas.

It is obvious that the development of the ionization should be described by a system of equations of kinetics and gas dynamics. For a plane SW this system is written as follows:

The equation of the ionization kinetics:

$$\partial (n_e v)/\partial x = S_e \tag{1.1}$$

The equation of the energy balance of the electrons:

$$\partial ({}^3/_2 n_e v T_e)/\partial x + T_e n_e \partial v/\partial x = \sum_i Q_i. \tag{1.2}$$

Here x is the distance from the SW front, v is the velocity of the gas, n_e and T_e are the concentration and temperature of the electrons, and S_e is the source of electrons due to the aggregate of the various elementary processes. The quantities Q_i correspond to the various processes of heating and cooling of the electron gas resulting from elastic and inelastic collisions. The convective term $T_e n_e \partial v/\partial x$ can be neglected, excluding the region directly adjacent to the SW front. Unlike in a SW, in a completely ionized plasma the electron thermal conductivity in (1.2) is unimportant. However, for a SW of sufficient amplitude, the electron thermal conductivity also plays a part in the propagation of the SW in an un-ionized gas (see Sec. 4.4).

The gas dynamics equations expressing the laws of conservation of the fluxes of mass, momentum, and energy, are of the form

$$\begin{gathered}\rho_1 V_1 = \rho v, \quad p_1 + \rho_1 V_1^2 = p + \rho v^2, \\ \frac{\partial}{\partial x}\left[\rho v \left(h + \frac{v^2}{2}\right)\right] = -Q_R.\end{gathered} \tag{1.3}$$

Here ρ is the density, p is the pressure, h is the specific enthalpy of the gas, and Q_R are the energy losses resulting from the emission of radiation. The subscript 1 marks quantities referring to the state of the gas ahead of the compression jump.

The system of equations (1.1)—(1.3) is complicated. This is connected with the fact that the quantities S_e, Q_i, and Q_R depend to some extent on the distribution of atoms over the excited states, as well as on the energy distribution of the electrons which is not always Maxwellian. In addition, for SW in molecular gases it

*We also indicate reviews [7,8] which contain extensive material on the rate constants of various reactions essential for the investigation of nonequilibrium effects behind weak SW in molecular gases.

turns out to be essential to write down kinetics equations of the type (1.1) also for the other components.

In accordance with the discussion we shall consider in the review problems of the ionization kinetics in a plasma, the mechanisms of the initial ionization and the structure of the relaxation region. In the concluding section we discuss the radiation of the nonequilibrium region.

2. IONIZATION KINETICS IN A LOW-TEMPERATURE PLASMA

2.1. Ionization and Recombination in an Atomic Plasma in Collisions with Electrons

In early papers it was assumed that the ionization occurs from the ground state of the atom. Accordingly ionization coefficients by electron impact, collision with an atom or ion, and photoionization coefficients were differentiated. In reality each act of ionization is the result of a large number of collision and radiation processes in which the bound electron, acquiring and losing energy, passes gradually through a large number of excited states. Therefore the use of the above-mentioned various coefficients of ionization (recombination) makes sense only in limiting cases when some elementary process dominates.

We shall write the rate of change of n_e in the usual manner:

$$S_e = n_1 n_e \beta - n_e^3 \alpha, \tag{2.1}$$

where n_1 is the concentration of electrons in the ground state and α and β are the recombination and ionization coefficients. The role of the various elementary processes affects the form of α and β. Let us consider the limiting case in which excitation and ionization by electron impact predominates.

In order to find α and β, one must know the populations of all the excited states of the atom which are determined from a solution of the system of nonstationary equations of the balance of particles at each of the levels. However, if one is not interested in very small time intervals from the beginning of the process (of the order of 10^{-8}–10^{-7} sec), then one can make use of the quasistationarity approximation of the excited states. It consists in the fact that states whose populations are small, $n_k \ll n_e$ and n_1, manage at each instant during the relaxation process to adjust to the relatively slow changes of the concentration of electrons and their temperature. This makes it possible to consider the system of stationary equations of the balance of particles in excited states of the atom and to obtain sufficiently general expressions for the coefficients α and β.

It is known that transitions of electrons between energetically close states are the most probable. Therefore the process of ionization (recombination) can be considered as some slow probability process of the type of Brownian motion in energy space. The ideas of a diffusion approximation in the recombination kinetics at low temperatures were developed in the paper of Belyaev and Budker.[10] However, in order to extend the range of problems the diffusion approximation must be combined with an account of the discrete nature of the energy spectrum of an atom.

The diffusion approximation in energy space was developed in[11-13] and a Fokker-Planck type equation in finite differences for bound electrons and a differential equation for free electrons were obtained. By solving it the distribution of atoms over the energy levels was obtained and the coefficients α and β were calculated with account of both collision and radiation processes, as well as of the possible violation of the Maxwellian energy distribution of the electrons.

When the ionization and excitation are due solely to electron impact, the approximate expression for β is of the form[13]

$$\begin{aligned} \beta^{-1} &= \beta_1^{-1} + \beta_2^{-1}\chi(E_2/T_e), \\ \beta_1 &= \Gamma F_1 \Lambda_1 \frac{(\mathrm{Ry})^{3/2}}{\sqrt{T_e}(E_1 - E_2)} e^{(E_2 - E_1)/T_e}, \\ \beta_2 &= \frac{2}{3\sqrt{\pi}} \Gamma \bar{\Lambda} \frac{\Sigma_i}{g_1} \left(\frac{\mathrm{Ry}}{T_e}\right)^3 e^{-E_1/T_e}, \\ \Gamma &= 4\sqrt{2\pi}e^4/\sqrt{m}\,\mathrm{Ry}^{3/2} = 1{,}7 \cdot 10^{-7}\ \mathrm{cm}^3/\mathrm{sec}; \end{aligned} \tag{2.2}$$

E_1 and E_2 are the energy levels of the ground and first excited states reckoned from the continuum, g_1 and Σ_i are the statistical weight of the ground state and the partition function of the residual ion,

$$\chi(x) = {}^4/_3\sqrt{\pi} \int_0^x e^{-t} t^{3/2}\, dt,$$

$$\begin{aligned} \chi(x) &\cong 1 - ({}^4/_3\sqrt{\pi})\, x^{3/2} e^{-x}, & x \gg 1, \\ \chi(x) &\cong ({}^8/_{15}\sqrt{\pi})\, x^{5/2}, & x \ll 1. \end{aligned}$$

The quantity F_1 takes into account the non-Maxwellian nature of the energy distribution of the electrons and will be discussed below. For a Maxwellian distribution $F_1 = 1$. Formula (2.2) makes it possible to calculate readily the ionization coefficient under various specific conditions.

The ionization coefficient depends naturally on the cross sections of the individual transitions. However, these quantities enter in (2.2) in combinations which are insensitive to the possible errors of the individual cross sections. This enables one to take into account the peculiarities of the individual transitions by means of a universal quantity, the so-called Coulomb logarithm for bound states, Λ_k, which depends on the ratio of the transition energy ΔE and T_e. The corresponding graph plotted on the basis of the presently available cross sections is shown in Fig. 1. The weak dependence of β on the cross sections of the individual transitions made it possible to take into account in (2.2) all Λ_k, $k \neq 1$, by introducing $\bar{\Lambda} \approx 0.2$. The most important transition $1 \rightarrow 2$ is taken into account by Λ_1. (In Sec. 5.1 we shall also make use of Λ_k, $k \neq 1$.)

Formula (2.2) is a good approximation to a more

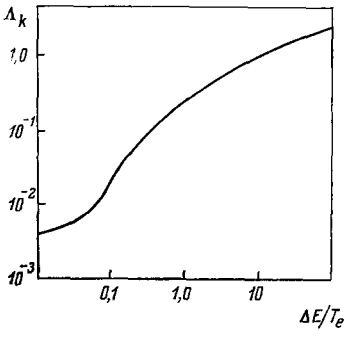

FIG. 1. Dependence of the Coulomb logarithm for bound states Λ_k on the relative energy of the transition $\Delta E/T_e$.

general expression obtained in[13] and is in fair agreement with experiment and with the results of machine solutions[14] of the system of equations of the kinetics of the excited states.

Let us discuss the limiting cases of high and low temperatures.

At high temperatures (the ionization energy of the first excited state is comparable with the kinetic energy of the electrons) one can assume that each excited atom appearing in the ionization process will be immediately ionized. In this case the rate of ionization is determined by the excitation rate

$$\beta = \langle z_{12} \rangle = \sum_{n \geqslant 2} \langle w_{1n} \rangle = \beta_1, \qquad (2.3)$$

where $\langle w_{1n} \rangle$ is the excitation probability $1 \to n$ averaged over the electron distribution function. This approximation of "immediate ionization" in the problem of the relaxation behind the shock wave was used in a number of papers starting from[9]. In the case of high T_e the approximate value of the sum (2.3) corresponds to the first term in formula (2.2).

Only the highest excited states are ionized directly at low temperatures. The population of the first excited states remains, therefore, during the relaxation process close to its Boltzmann values corresponding to T_e. This makes it possible to go over in the Fokker-Planck equation from a discrete to a continuous spectrum not only in the region adjoining the continuum[10,15] but in the entire energy range. Then,

$$\beta = \beta_2, \quad 2(3/2)^{3/2} \sqrt{T_e/\mathrm{Ry}} \ll 1. \qquad (2.4)$$

The factor F_1 in (2.2) appears as a result of taking into account the possible violation of the Maxwell distribution, since each act of excitation by electron impact means a simultaneous displacement of the free electron into the region of lower energies. The Maxwellizing factor are the interelectron collisions, however their role in the region of higher energies may turn out to be insufficient. An expression has been obtained for F_1

$$F_1 = \frac{1}{C} \frac{\sqrt{1+4C}-1}{\sqrt{1+4C}+1} \cong \frac{1}{1+C},$$
$$C = 2 \frac{n_1}{n_e} \cdot \frac{T_e}{E_1 - E_2} \cdot \frac{\Lambda_1}{\lambda},$$

where Λ_1 is the Coulomb logarithm for interelectron collisions, $\lambda = \ln(9T_e^3/8\pi n_e e^6) + 1$. Under characteristic conditions $\lambda \cong 10$, and $\Lambda_1 \cong 0.01-0.05$.

Thus, formula (2.2) combining both diffusion considerations as well as an account of the discreteness of the atomic levels has clear limiting expressions determining their limits of applicability and is in fair agreement[13] with experiment. As an illustration we present in Fig. 2 the values of β for an argon and potassium plasma. As one would have expected, for the potassium atom which has a relatively uniform density of levels the usual diffusion approximation has a larger region of applicability. On the other hand, the immediate ionization approximation works well for argon. In Fig. 2 the curves corresponding to the various degrees of ionization illustrate the influence of the non-Maxwellian nature of the electrons on the value of β.

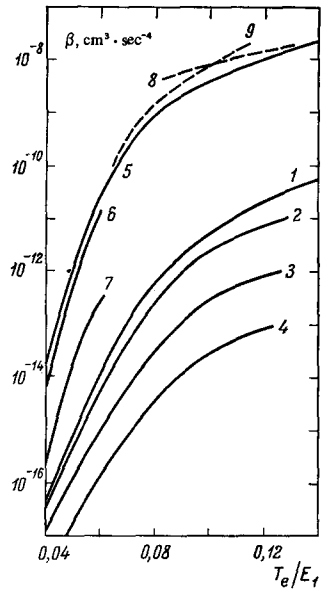

FIG. 2. Dependence of the ionization coefficient β on the relative temperature (E_1 –ionization energy). Argon, Eq. (2.2) for various degrees of ionization: $1-\alpha = 10^{-2}$, $2-10^{-3}$, $3-10^{-4}$, $4-10^{-5}$. Potassium, Eq. (2.2),–curve 5; curves 8 and 9–limiting cases of β_2 and β_1. Potassium in a mixture with argon (the product of the thickness of the plasma layer and the ratio of potassium atoms to argon atoms was taken to be 10^{-4}), Eq. (2.5) for various n_e: $6-n_e = 10^{13}$, $7-10^{12}$ cm^{-3}. In plotting curves 6–9 it was assumed that $F_1 = 1$.

2.2. The Effect of Radiation and Interelectron Collisions on the Kinetics of Ionization and Recombination

We present below an expression for β augmented by an allowance for radiation and for interatomic collisions. Of the interatomic collisions we have only retained $1 \rightleftarrows 2$ transitions, and the radiative transitions between excited states have been taken into account approximately (a more general expression for β can be found in[13]). We have

$$\beta^{-1} = (\beta_1 \xi_1)^{-1} + (\beta_2 \xi_2)^{-1} \chi(E_R/T_e),$$
$$\xi_1 = \frac{n_e \langle z_{12} \rangle^0 F_1 + n_a \langle z_{12}^a \rangle}{n_e \langle z_{12} \rangle^0 F_1}, \qquad (2.5)$$
$$\xi_2 = \frac{n_e n_1 \langle z_{12} \rangle^0 F_1 + n_a^2 \langle z_{12}^a \rangle}{n_e \langle z_{12} \rangle^0 F_1 + A_{21}^* + n_a \langle z_{12}^a \rangle} \cdot \frac{1}{n_2^0(T_e)}.$$

In (2.5) as before [as well as in (2.2)] the first term remains in the "immediate ionization" approximation and the second term characterizes the rate at which the electron passes through excited states. Therefore ξ_1 reflects the increase in the number of acts of excitation from the ground state due to interatomic impacts [$n_e \langle z_{12} \rangle^0$ and $n_a \langle z_{12}^a \rangle$ are the rates of the $1 \to 2$ excitation by an electron and an atom and $\langle\ \rangle^0$ indicates averaging over the Maxwell distribution of the electrons]. The factor ξ_2 represents approximately the ratio of the population of the second level n_2 with account of the interatomic collisions and the emission to the Boltzmann value $n_2^0(T_e)$; $\langle z_{21} \rangle^0$ and $\langle z_{21}^a \rangle$ are the efficiencies of impacts of the second kind, $A_{21}^* = A_{21}\theta_{21}$–is the emission probability with account of reabsorption (see Sec. 3.2). By the same token the factor ξ_2 takes into account the effect of the additional processes taken into account on the rate of the step-like ionization. The function $\chi(E_R/T_e)$ is responsible for a decrease in the rate of ionization resulting from the "counter" process–the emission of strongly excited states. For E_R we have the formula[13]

$$E_R \cong \mathrm{Ry} \cdot n_e^{1/4} (\sqrt{\pi}\, e^4 \bar{\Lambda}/\mathrm{Ry} \sqrt{m T_e}\, C_1)^{1/4},$$
$$C_1 \cong (3 \div 4) \cdot 10^{10} \ \mathrm{sec}^{-1}.$$

Formula (2.5) demonstrates graphically the nature of the influence of the interatomic collisions and radiative processes on the rate of ionization.

Radiative processes exert an influence on the kinetics for small n_e. The factors ξ_2 and $\chi(E_R/T_e)$ take into account radiative transitions between the lowest excited state and the ground state, as well as between excited states. In[16] in considering recombination allowance is made for factors corresponding to the appearance of ξ_2; an analog of $\chi(E_R/T_e)$ is in fact introduced in[17]. It is obvious that the regions of the applicability of the results of these papers are different (high and low temperatures respectively).

The relation between the ionization coefficients β and the recombination coefficients α is of the form

$$\beta = \mathcal{K}_1 \alpha n_1 \Pi^{-1}, \quad \Pi = \xi_1/\xi_2, \tag{2.6}$$

where $\mathcal{K}_1$ is the ionization equilibrium constant. Obviously the emission and collisions of heavy particles have a different effect on α and β. Behind a strong SW recombination becomes usually appreciable only for large n_e when collisions with electrons dominate the kinetics. Then, since $\Pi \to 1$ and $\xi \to 1$, $\beta = \mathcal{K}_1 n_1 \alpha$.

Let us draw attention to the limitations in using the above formulas. In (2.5) attention has only been paid to interatomic collisions of the following type:

$$X + X \rightleftarrows X^* + X. \tag{2.7}$$

No allowance is made for the processes of associative ionization and dissociative recombination

$$X + X \rightleftarrows X_2^+ + e, \tag{2.8}$$

$$X + X^* \rightleftarrows X_2^+ + e. \tag{2.9}$$

These processes will be discussed in subsequent sections.

Account of the radiative processes does not, of course, reflect phenomena connected with the presence in the plasma of large gradients of radiation density. Thus, for example, "illumination" by an intensely emitting equilibrium gas can accelerate the ionization in the relaxation zone. The appropriate generalization is considered in Sec. 3.2.

Ionization from the ground state and recombination with the direct formation of an atom in the ground state can become appreciable at high temperatures. These processes are not step-like and are readily taken into account. Their contribution to the change in the electron concentration is summed with the resulting contribution of the step-like processes.

2.3. Energy Balance of the Electrons

In an atomic plasma relaxation processes are described by three characteristic quantities: the ionization relaxation time τ, the relaxation time of excited states (to the quasistationary value) τ_k, and an analogous relaxation time of the electron temperature τ_T. These quantities usually satisfy the inequalities $\tau_k \lesssim \tau_T \ll \tau$.

The quasistationary nature of the excited states was discussed at the beginning of this section. The quasistationary nature of T_e has the same meaning physically and is due to the small energy contribution of the electrons to the enthalpy. After a time τ_T the temperature T_e "forgets" its initial value and is determined by the local energy balance:

$$^3/_2 T_e S_e + Q_{in} - Q_{el} = 0. \tag{2.10}$$

In (2.10) the sum of the energy sources ΣQ_i [Eq. (1.2)] is written in the form of a difference of the energy losses of electrons in inelastic collisions Q_{in} (excitation, ionization) and of heating by elastic collisions with atoms and ions Q_{el}. Inasmuch as the large energy losses of the electrons Q_{in} are compensated by the relatively slow heating by elastic collisions, T_e behind the front turns out to be considerably lower than the temperature of the atoms and ions T_a. This has already been explained in[9].

If the interatomic collisions are unimportant in the kinetics, then it is convenient to represent Q_{in} in the form

$$Q_{in} = E_1 S_e + Q_R + Q_{st}, \tag{2.11}$$

where $E_1 S_e$ are the energy losses to ionization, Q_R are the radiative energy losses, and Q_{st} are energy losses for the maintenance of the quasistationary population of excited states

$$Q_{st} = \sum_k (E_1 - E_k)\, \partial n_k v/\partial x.$$

In practice Q_{st} is inappreciable in cases when the first excited state is separated from the ground state by a considerable energy interval (for example in the inert gases). In the opposite case (for example, for nitrogen and oxygen atoms) one must take into account the terms of the basic electron configuration.[18,19]

In order to calculate Q_R one needs the nonequilibrium values of the population of the radiating states. In Sec. 5.1 we present the appropriate formulas obtained in solving a system of balance equations of excited atoms in the diffusion approximation (see above).

When the interatomic collisions influence the ionization kinetics the form of the notation of Q_{in} (2.11) must be changed. For instance, whereas in the immediate ionization approximation the role of interatomic collisions reduces to (2.7), during the first stages of relaxation

$$Q_{in} = E_1 n_e \langle z_{12} \rangle + E_2 n_a \langle z_{12}^a \rangle + Q_R. \tag{2.12}$$

It is, however, possible that interatomic collisions ionize effectively the excited states [process (2.8)] and the electron appearing has a certain energy E. Then,

$$Q_{in} = (E_1 - E_2)\, n_e \langle z_{12} \rangle - E n_a [\langle z_{12}^a \rangle + \langle z_{12} \rangle] + Q_R. \tag{2.13}$$

The actual course of the processes is often not completely clear, since all cross sections for interatomic collisions are not known. We note, however, that during the first stage of relaxation when the interatomic collisions are important, a knowledge of the exact values of T_e is not always essential for calculating the relaxation times. Such is, for example, the case behind a SW in inert gases.

In molecular gases molecular components may be present because of the incomplete dissociation during the initial stage of relaxation. In collisions of electrons with molecules rotational, vibrational, and electronic degrees of freedom may be excited. The mechanisms of

these processes are, as is well known, very diverse (see, for example[21,22]).

The rate of energy exchange in collisions of the electron with a molecule accompanied by a change of the rotational energy of the latter has been calculated in[23]. This process is of little importance under the conditions behind strong SW.

The direct excitation of vibrational levels of diatomic molecules in collisions with slow electrons is difficult because of the sharp mass difference of the colliding particles and the relatively large energy transferred. However, in certain instances (for example, N_2, CO[24]) a peculiar capture process of the slow electron by the molecule with the formation of an unstable negative ion is observed. After its "decay" the molecule may turn out to be in a state with a vibrational quantum number which differs by several units from the initial quantum number. This is accompanied by a considerable change in the electron energy (we recall that for N_2 the vibrational quantum $\hbar\omega = 0.29$ eV).

For the rate of energy exchange between the electrons and molecules we have the approximate formula[25]

$$Q_v = \hbar\omega P_{10}(T_e)(\varepsilon_v - \varepsilon_e)(\varepsilon_v + \varepsilon_e + 1), \qquad \varepsilon = (e^{\hbar\omega/T} - 1)^{-1}. \quad (2.14)$$

A more exact expression can be found in[26]. For a nitrogen molecule

$$P_{10} = 4{,}5 \cdot 10^{-9} \exp(-10^4\,°\mathrm{K}/T_e)\ \mathrm{cm}^3/\mathrm{sec}$$

is the average deactivation cross section of the first vibrational level of N_2.[25] Q_V plays an appreciable part in the energy balance of the electrons and in the vibrational relaxation behind strong SW in air.[19]

Energy losses for the excitation of electron states in molecules are taken into account in the usual way. As a rule they are not large.

In completing the discussion of the role of molecular components, we shall note the electron heating mechanism due to associative ionization [(2.8)—(2.9)]. The electron appearing in associative ionization takes on an energy $\sim T_a$.[27] Correspondingly, the electron disappearing in dissociative recombination carries away on the average an energy 3/2 T_e. The contribution of these processes (Q_{ai}) to the energy balance is

$$Q_{ai} = {}^3/_2 T_a S_{ai} - {}^3/_2 T_e S_{dr}, \quad (2.15)$$

where S_{ai} and S_{dr} are the rates of the direct and inverse processes respectively; their explicit form is discussed in 3.1. The quantity Q_{ai} plays an appreciable role only at the very beginning of the relaxation.

As an illustration we present in Fig. 3 the energy balance behind a SW in air (for the profiles of the fundamental parameters of the plasma see Fig. 24 below).[26] At the beginning of the relaxation the electrons are heated intensely by collisions with vibrationally excited molecules, a fact which compensates for energy losses to excitation and ionization. With the passage of time the molecules dissociate and the atomic low-lying excited states having accumulated up to then a considerable amount of energy, begin to heat the electrons by impacts of the second kind. We note that the elastic collisions with ions which play the main part in heating in inert gases are here almost unnoticeable.

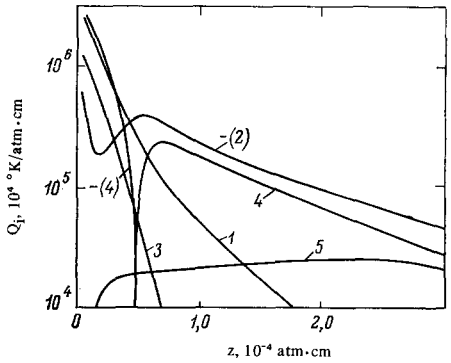

FIG. 3. The contributions of various processes to the energy balance of the electrons of a SW in air; $V_1 = 10$ km/sec, $p_1 = 0.1$ mm Hg, and $z = p_1 x$. Curves: 1—Q_V; 2—$E_1 S_e$; 3—Q_{ai}; 4—energy losses to excitation and heating by collisions of the second kind, 5—Q_{el}.

X	Ar	Xe	Kr [32]	Ar [33]
σ_0, cm²/eV	$1{,}2 \cdot 10^{-19}$	$1{,}8 \cdot 10^{-20}$	$1{,}4 \cdot 10^{-19}$	$2{,}5 \cdot 10^{-20}$

3. IONIZATION DURING THE FIRST STAGE OF RELAXATION

It was noted above that during the first stage of relaxation, when the electron concentration is still small, ionization by electron impact cannot ensure the required rate of generation of charged particles. Let us consider various processes that can be the reason for the initial ionization.

3.1. Ionization in Atom-Molecule Collisions

The cross sections for ionization from the ground state in atom-molecule collision at near-threshold energies are not large—10^{-20} cm².[21,28] This process is, therefore, insufficiently efficient to explain the initial ionization.[29] Weymann[30] proposed that behind a SW in inert gases the ionization in atom-atom collisions may be step-like. Because of a decrease of the threshold energy (in the immediate ionization approximation) the collisions (2.7) can be sufficiently efficient.

So far the theory of atomic collisions still does not make it possible to calculate the cross section for process (2.7). However, the necessary information can be obtained from an analysis of certain experiments in shock tubes. Microwave measurements[31-33] yield a linear increase of n_e behind the front. From these data one can obtain the magnitudes of the averaged cross section and of the threshold energy. The latter has turned out to be close to the first excitation potential, a fact which is serious evidence in favor of a step-like ionization. It is assumed that the rate of ionization is determined by the rate of excitation, and the excitation function depends linearly on the energy. In the Table we present the values of the slope of the excitation function σ_0 (in cm²/eV) obtained by various authors.

The conditions of the experiments of Kelly[32] and of McLaren and Hobson[33] are similar—$M_1 \simeq 7-10$ and $p_1 = 1$ mm Hg. In[33] there are considerations favoring a view that Kelly's data are overestimated.

Unlike the papers mentioned, in[34] use was made of an optical interferometer to measure the course of n_e, and $M_1 = 15-18$. The authors note that they could not choose an energy dependence of the atom-atom excitation cross section which would ensure agreement with experiment for different M_1. Unfortunately no preliminary numbers of any sort are cited in[34].

Apparently the data of the Table really characterize the process (2.7). The role of radiation could hardly have been large and the impurity level did not exceed 10^{-6}. Estimates[35] attest to the applicability of the "immediate ionization" approximation under the conditions of[32,33]. However, it has been assumed in[35] that resonance radiation is fully reabsorbed. This requirement is equivalent to the radiative transitions $2 \rightarrow 1$ being almost completely compensated by the counter process caused by the absorption of $1 \rightarrow 2$ radiation [see (2.5)]. Thus, assuming that the rate of the initial ionization is completely determined by atom-atom collisions, we admit implicitly an appreciable influence of radiative transfer processes.

In molecular gases the initial ionization may be due to a very efficient mechanism—associative ionization, (2.8) and (2.9). The efficiency of these processes is explained by the large magnitude of the cross section and by the relatively small activation energy of the reaction (thus, the minimum threshold in the case $N + N \rightarrow N_2^+ + e$ amounts to 6.3 eV, and in the case $N + O \rightarrow NO^+ + e$—to 2.8 eV). In their application to weak SW in air the processes of associative ionization were first discussed in detail by Lin and Tear.[36]

Assuming for simplicity that the molecular ion is produced in the electronic ground state, we shall write down the rates of generation of charged particles:

$$S_e = S_{ol} - S_{dr} = n_1 \sum_k \beta_k(T_a) n_k - n_e n_2^+ \sum_k \alpha_k(T_e), \qquad (3.1)$$

$$\bar{\alpha} = \sum \alpha_k, \quad \bar{\beta} = \sum \beta_k n_k / \sum n_k, \qquad (3.2)$$

where n_k is the concentration of atoms on the k-th excited level, and n_2^+ is the concentration of molecular ions. Expression (3.1) extends in an obvious way to the case of interaction of atoms of different elements.

The literature data on the rates α_k and β_k (i.e. on the final states of the reaction products) are limited. In theoretical work use is made of model considerations whose range of applicability remains unclear. Only the summary efficiencies of the reactions $\bar{\alpha}$ (decaying plasma) and $\bar{\beta}$ (ionization relaxation behind a SW) have been determined experimentally in nonoverlapping temperature ranges. Inasmuch as the measurements are usually carried out under nonequilibrium conditions, the calculation of $\bar{\alpha}$ from a known $\bar{\beta}$ (and vice versa) requires care (the relations of detailed balance can only be written for α_k and β_k).

Apparently a strongly excited atom appears in dissociative recombination of an inert gas molecular ion.[42] Metastable atoms of the fundamental configuration are formed in the case of N_2^+, O_2^+, and NO^+ [in the case O_2^+ the atom $O(^1D)$][43]. In Fig. 4 we present experimental data on the dissociative recombination coefficient in nitrogen (for an analogous summary graph for NO^+ see[44]). Curves 5 and 6 are obtained by recalculating the values of $\bar{\beta}$ under the assumption that the distribution of atoms over excited states was an equilibrium

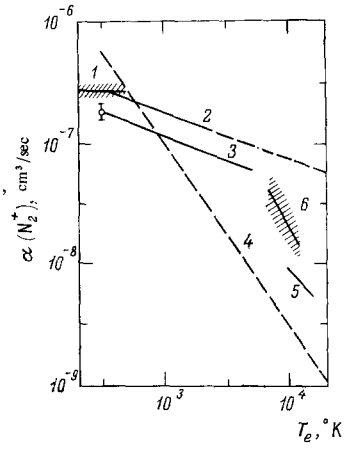

FIG. 4. Dependence of the coefficient of dissociative recombination of N_2^+ on T_e. Data of microwave measurements in a decaying plasma. Curves: 1—[37], 2—[38], 3—[39]. Values of α obtained from the rate of associative ionization in SW: 4—[36], 5—results of the processing [19] of infrared radiation oscillograms [40] behind a SW in air (see Fig. 19), 6—results of measurements [41] in a mixture of $Ar + N_2$.

distribution in accordance with the atomic temperature. The dashed portion of curve 2 in Fig. 4 corresponds to extrapolation of the data[38] to higher temperatures. The contradiction between 2 and 5 reflects a lack of information concerning the states of the final reaction products. Thus, assuming that the main contribution to $\bar{\beta}$ is due to β_3, we obtain α_3 close to the dashed curve.

3.2. Ionization Due to Radiative Transfer

The gradients of the plasma parameters behind the SW are not large, and in this connection molecular transfer phenomena do not play an important part. The transfer of radiation which has larger free paths can affect the course of the relaxation in two ways. The SW radiation may precede the wave and produce ahead of the front excited atoms and electrons. These particles are carried into the relaxation zone, accelerating the process of initial ionization. In addition, the radiation of the equilibrium region is absorbed in the relaxation zone, a fact which also accelerates the approach to equilibrium. In this, as in the other case, the transfer of radiation in the lines and in the continuum may be important.

In the case of a plane wave the source of excited atoms due to radiation transfer in the spectral line is written in the following form[45]:

$$B_k(x) = -A_{k1}\left[n_k(x) - \int_{-\infty}^{+\infty} n_k(\xi) K_k(x, \xi)\, d\xi\right], \qquad (3.3)$$

where A_{k_1} is the probability of the spontaneous transition $k \rightarrow 1$, and $n_k(x)$ is the population of the emitting level at the point x. The first term in (3.3) characterizes the emission, the second—the absorption of radiation from the remaining volume of gas. $K_k(x, \xi)$ is the probability that a photon emitted in a volume element with the coordinate ξ will be absorbed at x. $K_k(x, \xi)$ is determined by the emissivity of the gas and by the spectral absorption coefficient $k_\nu(x)$.

Thus, to find the rate of ionization with account of radiative transfer requires the solution of a system of integro-differential kinetics equations. This is due to the fact that radiative transfer couples plasma volumes remote from one another.

In certain instances the entire volume occupied by the plasma divides into several weakly inhomogeneous regions which differ sharply from one another (for example, the plasma ahead of and behind a SW). Then the

source B_k can be transformed into another form which admits further simplification. Let us divide the gas volume into two regions ("hot" and "cold" gas). Let us assume that within the limit of its emission lines the hot gas is black at some temperature T. Then one can write for the source of excited atoms in the cold gas the expression[18]

$$B(x) = A[n^0 - n(x)]\theta(x) - \int_0^\infty d\xi A[n(x) - n(\xi)]K(x, \xi). \quad (3.4)$$

The first two terms in (3.4) take into account exchange by means of radiation between the cold and hot gas—"irradiation" of the cold volume by the hot volume and the inverse process of "emission." n^0 is the Boltzmann concentration at T, and $\theta(x)$ is the probability of emission beyond the limits of the volume V occupied by the cold gas, as usual in describing transfer in a weakly inhomogeneous medium.[46] In this review it makes sense to consider lines of the dispersion contour, since photons which correspond to the "tails" of the line have larger mean free paths. If the "cold" gas can be considered to be optically homogeneous, then

$$\theta(x) \cong (2 + 3\sqrt{\pi k_0 x})^{-1}, \quad (3.5)$$

where k_0 is the absorption coefficient at the center of the line.

The last term in (3.4) is only appreciable when the "cold" gas is strongly inhomogeneous. It takes into account exchange by means of photons occuring within its volume. The articles[47] are devoted to problems connected with the transfer of radiation in the spectral line in an inhomogeneous medium.

Analogously one can write down the source of electrons due to radiative transfer in the recombination continuum. In (3.4) n_k is replaced by n_e^2, and A_{k_1} by α_{e_1} where α_{e_1} is the coefficient of radiative recombination to the ground state.

a. **Precursor radiation.** The effect of precursor radiation on the state of the gas ahead of the front of the SW was first considered by Zel'dovich and Raĭzer[1,2] in connection with the problem of the luminosity of a high-intensity SW front. The heating of the gas ahead of the front was considered in this work. Nonequilibrium effects ahead of the SW front were considered in[48]. It was shown that the precursor radiation produces a wave of excited atoms ahead of the front; the concentration of the atoms may approach the Boltzmann concentration at the equilibrium temperature T_{eq}.

In[48] use was made of the circumstance that in a region not too close to the front one can neglect the last term in (3.4). The equation for n_2 was solved with account of extinction and flux drift. As a result $n_2(x)$, being close to a Boltzmann distribution at the temperature of the hot gas behind the front T_{eq}, decreased slowly on going away from the front. It was also noted in[48] that the photoionization of the excited atoms leads to the appearance of an appreciable concentration of electrons at large distances from the front.

The electron concentration ahead of the front has been calculated in[48]. At large distances it is determined by the photoinoization of the excited atoms, and at small distances—by the photoionization of atoms in the ground state. The latter effect increases appreciably with increasing SW velocity. A considerable number of papers has been devoted to phenomena connected with the precursor radiation; discussion of these would lead us outside the limits of this review. We shall only draw attention to the work of Murthy[51] who considered the same problem in detail and obtained similar final results.

The results obtained for a plane SW can be used to interpret phenomena in shock tubes only as a limiting case corresponding to the ideal reflection of radiation from the walls. The other limiting case—the absence of reflection—was considered in[49]. The absorption by the walls weakens the primary irradiation by a factor

$$f(y) = 1 - y^{3/2}(1 + y^2)^{-3/4}, \qquad y = x/R. \quad (3.6)$$

The expression for $\theta(y)$ also changes. To sum up, for $y \gtrsim 1$ the concentration of electrons and excited atoms decreases considerably.

b. **Ionization behind the SW front due to radiation transfer.** The problem of the effect of radiation on the initial ionization has been discussed in the literature repeatedly starting with[9,50]. The rate of the initial ionization due to radiative transfer in the spectral lines has been calculated in[52] with a series of assumptions. Since the immediate ionization approximation works well behind the front, one can confine oneself in (3.4) to a consideration of "irradiation" from the equilibrium region only. If, in addition, one considers the relaxation zone to be optically uniform (we neglect Stark broadening and the compression of the gas which are only important in a nanow layer), then the rate of the initial ionization is of the form[52]

$$B_l(x) = \sum_k A_{k_1} n_k^0(T_{eq})\,(3\sqrt{(k_0)_k \pi(\Delta x - x)})^{-1}, \quad (3.7)$$

where the sum is taken over all transitions to the ground state, Δx is the relaxation length and x is measured from the equilibrium zone. In order to take into account absorption by the walls, (3.7) must be multiplied by $f[(\Delta x - x)/R]$.

The contribution of the recombination continuum to the electron source has been considered by Kuznetsov[53] and subsequently in a series of papers by other authors.[54,55] Assuming that the coefficient of photoionization depends weakly on the frequency, we obtain

$$B_c(x) = N(T_{eq})\varkappa\varphi[\varkappa(\Delta x - x)], \quad \varphi(y) = e^{-y} + y\,\mathrm{Ei}(-y); \quad (3.8)$$

$N(T_{eq})$ is the number of photons of frequency $\nu > \nu_i$ (ν_i is the limit of photoionization from the ground state) emitted by a unit area of a black body per second, and κ is the photoinoization cross section.

In Fig. 5 we compare the rates of initial ionization directly behind the front due to absorption of radiation and to atom-atom collisions. The atom-atom excitation cross sections have been adopted from[33] for argon and from[32] for xenon (Table I), and the probabilities A_{k_1}—from[56,57]. Resonance, van-der-Waals, and natural broadening was taken into account. The relaxation lengths were based on experiments[9,58,59].

The role of emission is appreciable for small and large M_1 and increases with decreasing p_1.

Emission in the spectral lines is dominant for small M_1. With increasing M_1 the temperature of the atoms

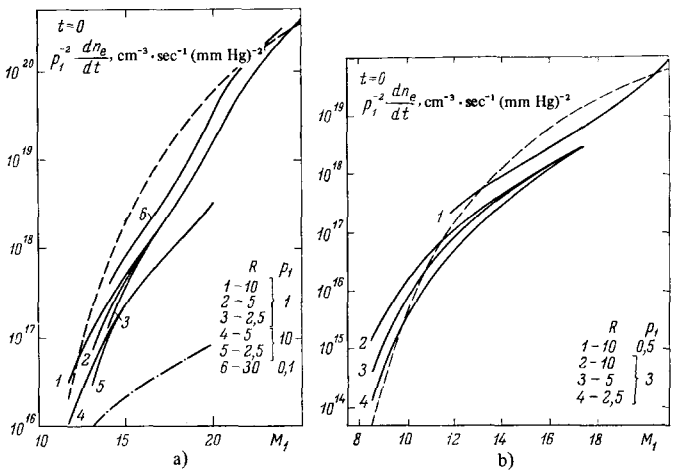

FIG. 5. Comparison of the rates of the initial ionization directly behind the front of a SW in argon (a) and xenon (b) in atom-atom collisions (dashed curve), with ionization of a 3×10^{-2} percent air impurity (dash-dot curve), and as a result of the absorption of the radiation. p_1 –pressure ahead of the front (mm Hg) and R is the shock-tube radius (cm).

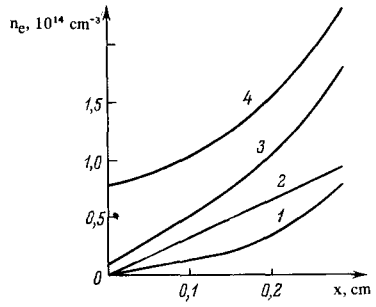

FIG. 6. The growth of n_e in the primary ionization zone behind a SW in argon, $M_1 = 20$, $p_1 = 1$ mm Hg. 2–ionization due to atomic collisions, 1–ionization due to absorption of radiation behind the SW front, 3, 4–growth of n_e with account of 1, 2, and the entry of electrons and excited atoms through the front (3 corresponds to complete absorption of the precursor radiation by the tube walls).

behind the jump begins to exceed more and more T_{eq} which determines the intensity of the emission. The intensity of the atom-atom excitation increases, therefore, more rapidly. On increasing M_1 further, the relaxation zone begins to transmit the continuum. Its role increases and becomes dominant. Figure 5 also shows the dependence of the initial ionization on R if one assumes complete absorption of the radiation by the walls of the stock tube. The effect of the walls is significant for $\Delta x \gtrsim R$.

Estimates analogous to those shown in Fig. 5 have also been presented by Zhikhareva and Tumakaev.[60] They considered a narrower range of conditions and did not take into account the contribution of electrons and excited atoms across the front (see below). Therefore the emission played a somewhat lesser role.

The radiation process is not binary and with decreasing p_1 the role of the emission increases. Small deviations from the binary nature in experimental data on the relaxation lengths ($p_1 \Delta x \neq$ const) can under certain conditions be connected with the effect of radiation. Such deviations from a binary nature (in the direction opposite to that due to recombination) are present in the results of Petschek and Byron (see Fig. 15 below).

Figure 5 still does not provide a full picture of the relaxation between impact and radiation processes. The contribution of the latter increases as one goes farther away from the front whereas the intensity of atom-atom collisions changes little. The effect of precursor radiation has also not been taken into account in Fig. 5. From this point of view it is useful to consider the profile $n_e(x)$ in the region of the primary ionization:

$$n_e(x) \cong 4v_1^{-1}\{\langle Z_{12}^a\rangle x + \int_0^x dx[B_l(x) + B_c(x)]\} + n_e(0). \qquad (3.9)$$

The role of the continuum in giving rise to $n_e(0)$ can be estimated assuming that the continuum photons not absorbed in the relaxation zone revert to it in the form of electrons. The spectral lines produce around the front a population of excited atoms which in an estimate from above can be taken to be Boltzmann-like at T_{eq}. Being ionized in the transition through the front, these atoms will make a contribution to $n_e(0)$.

The growth of n_e in the primary ionization zone is shown in Fig. 6 for a SW in argon in accordance with (3.9). Curve 4 corresponds to an estimate from above of the entry through the front. Curve 3 takes into account the entry under the most rigid assumption of nonreflecting shock-tube walls. It follows from Fig. 6 that the contribution of radiation to the primary ionization can be more appreciable than would follow from Fig. 5.

3.3. The Effect of Impurities on the Initial Ionization

In discussing the results of their measurements Petschek and Byron assumed that the initial ionization is due to impurities in the working gas. However, only for SW in the region $M_1 = 10$–12 can their experiments (with impurity levels of 5×10^{-5}, 2×10^{-5}, and 7×10^{-6}) be cited to confirm the initial assumption (see Fig. 16 below). It is remarkable, however, that to this end one must postulate a process taking place with the participation of the impurity which has a cross section $\sim 4 \times 10^{-14}$ cm^2 (this number has been obtained in[61] in processing the results of[9]). Petchek and Byron did not find such a process.

In the collision of heavy particles one of the most rapid ionization processes is the associative ionization of nitrogen and oxygen atoms. The dash-dot curve in Fig. 5 indicates the initial rate of generation of electrons in the presence of 3×10^{-2} percent air in argon. It is assumed that the N_2 and O_2 are completely dissociated. The dissociation time of N_2 behind the SW in argon for $M_1 \lesssim 15$ is considerably smaller than the length of the zone of ionization relaxation and becomes equal to the latter for $M_1 \simeq 20$. If there is not sufficient time for the nitrogen to dissociate fully then the heating of electrons in collisions with vibrationally excited molecules of N_2 may be considerable [see (2.14)]. Under these conditions the ratio $Q_v/Q_{el} \simeq 0.5\, \gamma_M/\alpha$, γ_M being the fraction of N_2 impurity.

Estimates of the influence of air impurity (the production of NO^+) were also made in[61] for SW in argon and in[62] for SW in a mixture of 0.9 Ar + 0.1 N_2. It was shown in[61] that if a special purification is not carried out (as, for example, in[71]), and the air impurity reaches 1 percent, then it may play an important part.

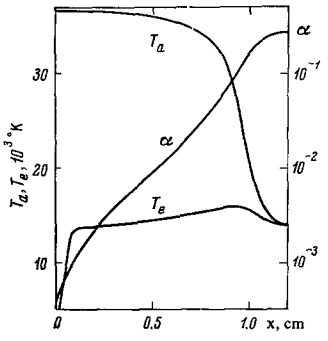

FIG. 7. Relaxation zone behind a SW in argon. $M_1 = 20$, $p_1 = 2$ mm Hg, and $T_1 = 300°K$.

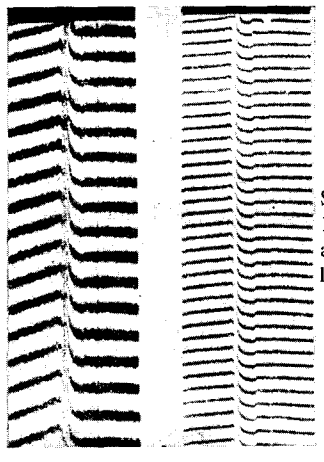

FIG. 8. Interference pattern of a SW in Ar + 0.5% H_2. $M_1 = 20.6$, $p_1 = 1.09$ mm Hg. Wavelengths $\lambda = 5300$ Å and 10,600 Å. The SW moves to the left.

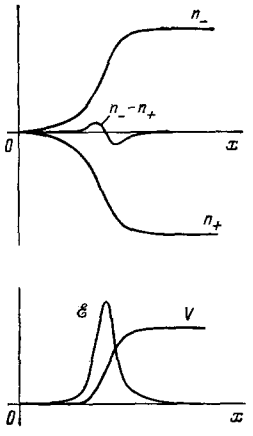

FIG. 9. Distribution of charges n_+, n_-, of the field $\mathcal{E}$, and of the potential V behind the SW front. x–distance from the front.

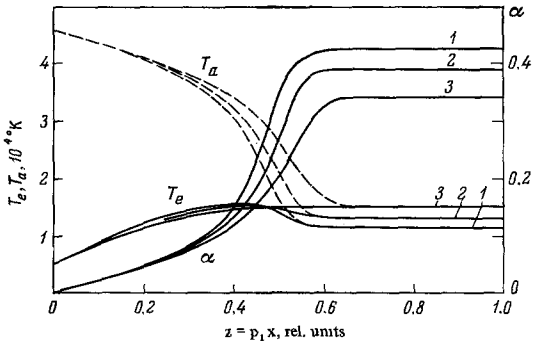

FIG. 10. Relaxation zone behind a SW in air. [18] $V_1 = 14$ km/sec, $T_1 = 300°K$. Pressure p_1: $1–10^{-4}$, $2–10^{-3}$, $3–10^{-2}$ atm.

Summing up the discussion of the mechanism of the primary ionization, one can note that in air and apparently in other molecular gases associative ionization is the determining process. In atomic gases interatomic collisions and emission compete. Processes in which impurities participate can play an appreciable role only at high concentrations of the latter.

4. STRUCTURE OF THE RELAXATION ZONE

4.1. Profiles of the Plasma Parameters in the Relaxation Zone

As a result of solving the system of kinetic equations in conjunction with the conservation equations one can obtain distributions of plasma parameters in the relaxation zone. In Fig. 7 we present a typical calculated case for a SW in argon. In Fig. 8 we present an interference pattern of a SW in argon on which the relaxation zone is clearly seen.* The relaxation occurs in two stages. Initially the degree of ionization α increases linearly, or somewhat faster if the emission is appreciable. Further, with increasing α the ionization by electrons whose rate is proportional to α becomes first and foremost; the dependence becomes exponential. It is therefore clear that if the initial ionization is very intense then the length of the zone Δx depends on its rate almost linearly. In the inverse case this dependence weakens and becomes logarithmic.

*The authors thank Professor I. I. Glass who kindly furnished the interference patterns.

We note that behind the SW the plasma is always quasineutral. Only where the gradients of n_e are largest does the possibility of the diffusion of electrons relative to the ions appear. As is seen from Fig. 9, adopted from the work of Bond,[63] the deviations from quasilinearity are small. For a discussion of these effects and estimates see[2]. More detailed calculations for SW in inert gases were carried out by Chubb.[64] The potential jump occurs at the point of the highest gradient of n_e. In[9] this fact was used to measure relaxation times.

In molecular gases the dissociation can take place more slowly than the ionization (for low SW velocities) or more rapidly; see Sec. 4.3. Figure 10 presents the profiles of the relaxation zone behind the SW in air for $V_1 = 14$ km/sec.[18] Under these conditions one can neglect the dissociation time. The splitting of the curves corresponding to different pressures, and consequently the deviation from a binary nature, is connected with an account of recombination.

A direct measurement of T_a is fraught with great difficulties. Thus the profile of the rotational temperature T_r of the excited electron state $B^2\Sigma_u^+$ of the N_2^+ ion behind a SW in nitrogen was determined in[65]. It turned out that the measured values of T_r exceed the calculated values of T_a. In fact, as a result of the nonadiabatic interaction of the states $A^2\Pi_u$ and $B^2\Sigma_u^+$ of the N_2^+ molecule the concept of T_r cannot always be used.[66]

The values of T_e reach the quasistationary level very rapidly; thereafter T_e varies slowly. Therefore the de-

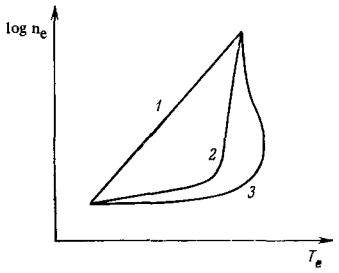

FIG. 11. Possible courses of development of the ionization.

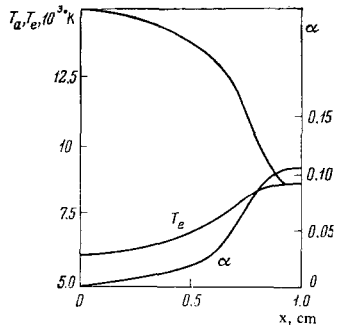

FIG. 12. Relaxation zone behind a SW in mercury vapor. M_1 = 10, T_1 = 200°C, and $n_1 = 1.0 \times 10^{17}$ cm^{-3}. T_e is given in the quasistationary approximation.

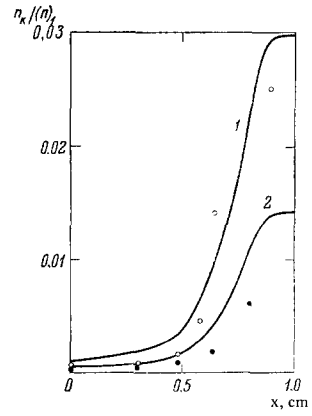

FIG. 13. Concentration of excited atoms behind a SW in mercury vapor (conditions of Fig. 12) relative to the concentration of atoms ahead of the front. 1–6 $^3P_1$, 2–6 $^3P_8$ level.

pendence on a very indefinite initial value is localized near the front where T_e does not influence the course of the relaxation. Calculations with various $T_e(0)$ carried out in[67] illustrate this fact. A rapid establishment of quasistationarity has been confirmed experimentally in[68].

It is sometimes convenient to depict the relaxation pattern in the $\{n_e, T_e\}$ plane. Along the curves in this plane (Fig. 11) there is a variation of the time with whose increase n_e increases. Three cases are possible: Case 1—the rate of ionization is so large that at each instant there is ionization equilibrium (n_e and T_e are related by the Saha equation). Only the slow energy exchange between the electrons and heavy particles prevents a more rapid establishment of equilibrium. Cases 2 and 3 correspond to an absence of local ionization equilibrium. Local overheating of electrons may then take place (case 3).

The nature of the $n_e(T_e)$ dependence depends to a considerable extent on the structure scheme of the terms of the atoms of the given gas. Cases 2 and 3 are realized in argon and air because of the presence of a considerable energy gap ($E_1 - E_2$); see Figs. 7 and 10. However, in mercury vapor, because of the very uniform distribution of levels in the spectrum, the ionization and excitation in collisions with electrons takes place rapidly so that there is time for a local equilibrium with a temperature T_e to be established. A so-called "two-temperature" plasma appears and the relaxation follows scheme 1 (Fig. 12). In Fig. 13 we present the experimental values of the concentrations of excited atoms[77] which are in good agreement with the Boltzmann values calculated for T_e. Inasmuch as recombination cannot be neglected in the entire zone, there appear specific deviations from a binary nature.

Located behind the recombination zone is a region filled with equilibrium plasma. The parameters of this plasma change incomparably more slowly than in the relaxation zone (Fig. 14). The plasma cools gradually, mainly due to the emission of radiation. A discussion of this effect is not part of the subject matter of this review (see, for instance,[4,18]). The local thermodynamic equilibrium is retained in a cooling plasma and only under certain conditions is it disturbed by the emission of radiation.

4.2. Comparison of Calculated and Measured Values of Relaxation Times in Atomic Gases

In Fig. 15 we present the results of Petschek and Byron obtained in argon at various pressures, as well as the calculated data of Morgan and Morrison[69] and Chubb.[64] Calculations[69] carried out with various values of the atom-atom excitation cross sections demonstrate well the sensitivity of Δx to the rate of the initial ionization—it is logarithmic. Chubb's calculation,[64] as the analogous calculation carried out by Hoffert and Lien[67] exceed the values measured in[9] for p_1 = 10 and 2 mm Hg by a factor of 2.5–3.0 and are in much better correspondence for p_1 = 50 mm Hg.

The results of Wong and Bershader[70] (Fig. 16) obtained by processing oscillograms of the profile $n_e(x)$ lie above the data of Petschek and Byron. They are, therefore, closer to the calculated curves.[64,69] The authors of[34,70] chose the atom-atom excitation cross section such as to satisfy the obtained n_e profiles (as was done in Fig. 14). Different values of the cross section were required for different M_1. This attests to the presence of an additional source of initial ionization. Small deviations from a binary nature appearing in Fig. 15 allow one to propose an effect of radiative transfer. However, as regards radiation from the equilibrium region, it was overestimated in[52]. In Fig. 16 we present the results of measurements of τ in argon with various impurity levels. It is difficult to establish a correspondence between τ and the impurity fraction γ.

The value of τ was measured behind a shock wave in xenon in[58 72-76]. In Fig. 17 we present the values of $p_1\tau$ obtained behind a normal SW by Smith[75] (optical measurements, $\gamma \sim 10^{-5}$), as well as preliminary results of interferometric measurements by Lazovskaya and Tumakaeva[58] ($\gamma \sim 10^{-2}$–10^{-3}). Regardless of the different impurity level, these are not in contradiction but are in poor agreement with the calculation of Chubb[64] in which the initial ionization was due to interatomic collisions.[32]

The literature contains results of measurements of

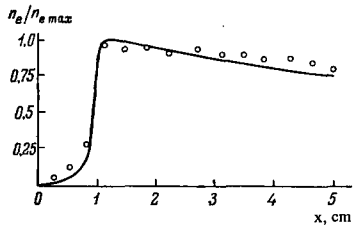

FIG. 14. Concentration of electrons behind a SW in argon. [34] M_1 = 18, T_1 = 300°K, p_1 = 3 mm Hg, $(n_e)_{max} = 1.8 \times 10^{17}$ cm^{-3}. [3] The circles mark the data of the processing of an interference pattern. The calculated curve was obtained by a choice of the magnitude of the atom-atom excitation cross section.

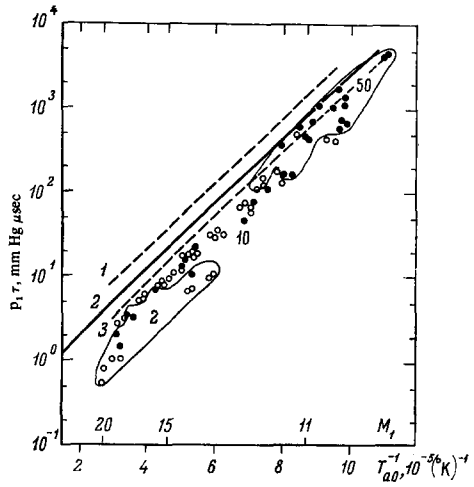

FIG. 15. Dependence of the product of the relaxation time τ in the laboratory system of coordinates and the pressure p_1 ahead of the front on the Mach number (the temperature behind the jump T_{a0}). Experimental data of Petschek and Byron, [9] pressures p_1 = 2, 10, and 50 mm Hg (indicated in the Figure). Two series of measurements are presented: O—Fig. 15 of [9], ●—Fig. 14 of [9]. Calculated data: 1, 3—Morgan and Morrison [69] with atom-atom cross sections 7.1×10^{-20} and 7.1×10^{-19} cm^2/eV respectively, Chubb, [64] cross section [19] 1.2×10 (sic!—Transl.) cm^2/eV.

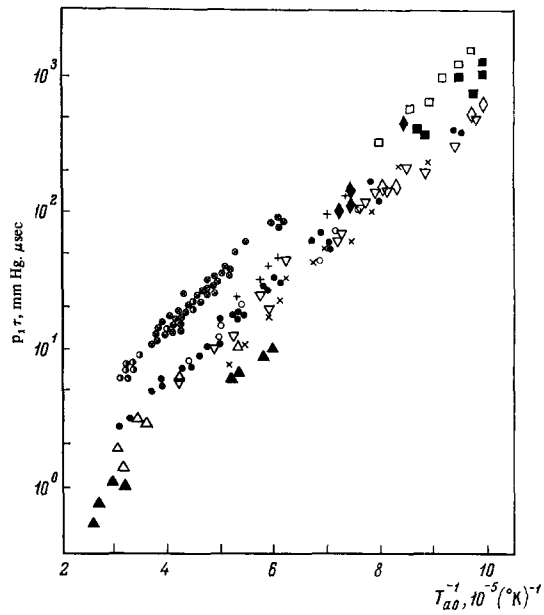

FIG. 16. Results of measurements of the relaxation time in argon (μsec) in the laboratory system for various initial pressures p_1 (mm Hg) and impurity levels γ. Data of [9]: Δ—p_1 = 2, $\gamma = 8 \times 10^{-5}$; O—$p_1$ = 10, $\gamma = 5 \times 10^{-5}$, ◇—$p_1$ = 50, $\gamma = 5 \times 10^{-5}$, □—$p_1$ = 50, $\gamma = 2 \times 10^{-5}$, ⊡—$p_1$ = 50, $\gamma = 7 \times 10^{-6}$; Δ, O, ◇—$\gamma \sim 10^{-3}$, p_1 = 2, 10, and 50 respectively. Reference [70]: O, O—$\gamma = 10^{-5}$, p_1 = 2, 5 respectively. Reference [71]: ▽—$\gamma = 3.5 \times 10^{-3} - 1 \times 10^{-2}$, p_1 = 5. Reference [61]: p_1 = 5, +—$\gamma = 3 \times 10^{-4}$, ×—$8 \times 10^{-3}$ respectively.

relaxation times in mercury vapor[58,77] (see the discussion of Figs. 12 and 13), potassium vapor,[78] and in a mixture of argon and cesium vapor.[79] Estimates for SW in argon with an admixture of cesium with the simplest scheme of kinetics show[80] that under the conditions of[79] the initial ionization is due to collisions of argon and cesium atoms. Calculations of the structure of the relaxation zone for SW in helium are given in[81].

In closing the discussion, we note that for SW in inert gases the relaxation lengths exceed the experimental values. As paradoxical as that is, the situation is considerably more satisfactory for air.

4.3. Ionization Relaxation Behind Strong SW in Molecular Gases

The development of ionization in molecular gases is marked by an interesting peculiarity illustrated in papers devoted to relaxation in air: the dependence of τ on V_1 passes through a maximum (Fig. 18) due to a change in the relaxation mechanisms.

For small V_1 the equilibrium degree of ionization α_{eq} is small. The ionization due to interatomic collisions does not affect the course of the relaxation of the gas. After a time τ, still during the initial stage of dissociation, the charged particles (electrons and molecular ions) reach quasiequilibrium with the relaxing gas.[36]

In the range $V_1 \sim 9$—10 km/sec (these values depend somewhat on p_1) α_{eq} increases by more than an order of magnitude. At the same time the effective temperature at which the ionization occurs changes insignificantly. This is due to the fact that the dissociation still continues in this range, and an increasing fraction of the enthalpy of the gas is lost to ionization. Thus an increase of V_1 and thereby of the initial enthalpy does not lead to an increase in the rate of ionization, whereas the number of charged particles (electrons and atomic ions) which one must obtain in the process of relaxation increases. Therefore τ also increases. For $V_1 > 10$ km/sec the dissociation is practically complete and α_{eq} depends relatively weakly on V_1. By virtue of this an increase in V_1 corresponds again to a decrease of τ.

The nonmonotonic nature of the dependence of $p_1\tau$ on V_1 was predicted in[82] and subsequently confirmed experimentally in[40,84]. In[82] molecular processes were practically neglected, a fact which did not make it possible to consider the intermediate range of velocities. The chemical, vibrational-dissociative, and ionization relaxation were considered jointly in[19]. The calculated radiation profiles in the infrared spectral region which provide direct information about the increase of n_e are in good agreement with the experimental profiles (Fig. 19). Therefore the relaxation times which increase in the interval V_1 = 9—10 km/sec by an order of

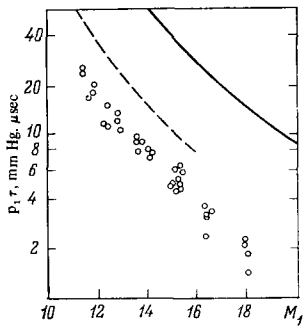

FIG. 17. Product of the relaxation time τ in xenon and of the initial pressure. Experimental points–[73], p_1 = 0.5 mm Hg. The dashed curve indicates preliminary results of measurements. [58] Calculated continuous curve–reference [64].

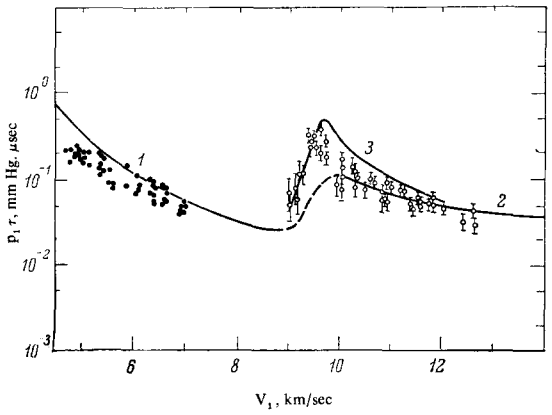

FIG. 18. The dependence of $p_1\tau$ on the SW velocity V_1 in air. Calculated curves: 1–[36], 2–[82], 3–[19]. Results of measurements: O–[83], O–[40].

magnitude are also in agreement with the measured values. Calculations of the relaxation for V_1 = 5–10 km/sec were carried out in[85].

The relationships observed in air will apparently also be fulfilled in other molecular gases, but the characteristic values of the velocities will, naturally, be different.

4.4. Stronger Shock Waves

New factors should manifest themselves in the relaxation mechanism for large Mach numbers. No experimental data are so far available under these conditions. With increasing M_1 in the region of M_1 = 30–40 the relaxation zone becomes extremely narrow and becomes comparable with the dimensions of a strong compression jump. It can therefore be assumed that an appreciable ionization will already appear in the jump. This effect was taken into account in the work of Chubb[64] who carried out calculations for SW in argon, krypton, and xenon. The structure of the jump was calculated by the Mott-Smith method (see, for example,[2]). However, the validity of using a bimodal velocity distribution of atoms for intensive inelastic collisions was not discussed. It was found that for the largest M_1 the relaxation zone exceeds only by a factor of three the length of the compression "jump."

For large M_1 and consequently at high temperatures there is an appreciable increase of the mutual influence of all regions of the SW due to radiative transfer. Clarke and Ferrari[54] took into account radiative transfer in the ionization continuum; the thickness of the discontinuity was ignored. The ionization was due to the absorption of radiation and to collisions with electrons. The mutual coupling of all regions of the SW was taken into account. The calculations were carried out for M_1 ~ 30 in argon and helium (Fig. 20). The precursor radiation gave rise to considerable ionization ahead of the front, increasing appreciably the enthalpy of the incoming flux. This led to a higher gas temperature directly behind the compression jump. Further the temperature fell as a result of the passage of ionization relaxation and radiative cooling. These effects are also discussed in a series of other papers; see the survey[86]. The work of[54] is of a model nature (this model is further developed in[87]) since the atom was assumed to have a two-level scheme and $T_e = T_a$. The difference between T_e and T_a was taken into account in[55] but, as in[54], radiative transfer in the lines was not considered. An attempt to take into account the effect of the L_α line on the SW structure in hydrogen was undertaken by Whitney and Skalafuris.[88] They took no account of the specific nature of the radiative transfer in the line, a fact which, as was shown in[89], led to erroneous conclusions.

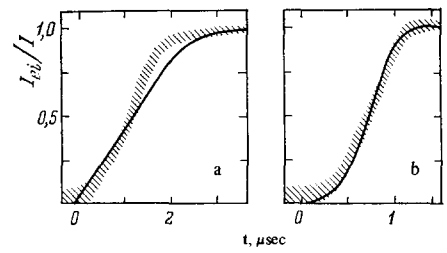

FIG. 19. Comparison of experimental [40] (shading) and calculated [19] reduced oscillograms of radiation with a wavelength $\lambda \sim 6\mu$ behind a SW in air. a–V_1 = 9.5 km/sec, p_1 = 0.2 mm Hg, b–V_1 = 10.9 km/sec, p_1 = 0.1 mm Hg.

So far we have considered phenomena behind the SW front in whose equilibrium region single ionization took place. With increasing SW velocity double (and with further increase of V_1 also multiple) ionization begins to play a part. The relaxation behind very strong SW, corresponding to multiple ionization, was considered in[105] in connection with the problem of the motion of meteorite bodies in the atmosphere. However, certain initial assumptions of[105] raise doubts. Thus, a Boltzmann distribution of atoms and ions over the excited states was assumed with the energy equations taking no account of losses for its support. Thermodynamically contradictory expressions were used for the coefficients of triple recombination and step-like ionization. No account was taken of the electronic heat conduction.

Magretova, Pashchenko, and Raĭzer[110] showed that the electronic heat conduction leads to a very strong overheating of the electron gas ahead of the wave front. As a result of this the ionization takes place principally before the jump. In order to calculate the kinetics of multiple (triple-quadrupole) ionization of a SW in air the authors of[110] used the model of ions with a "fractional," i.e. continuously varying charge.[2] This model leads to a simplification of the system of kinetics equations which now only contains equations for the electron

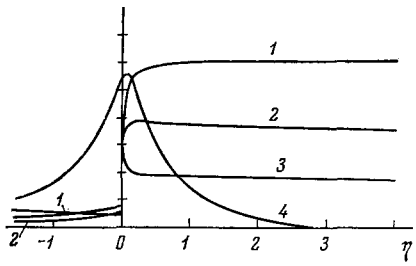

FIG. 20. Structure of a SW in argon. $M_1 = 28.9$, $p_1 = 10^{-3}$ atm, $T_1 = 300°K$. Curves—plasma parameters in relative units: 1—relative density $\rho/\rho_1 (\rho_4/\rho_1 = 12.3)$, 2—degree of ionization ($\alpha_4 = 0.720$), 3—temperature ($T_4 = 18{,}200°K$), 4—radiant energy flux relative to the total energy flux q ($q_0 = 0.111$). η—distance ahead of the SW front in free paths of the photon of the ionization continuum; 4 corresponds to the equilibrium state of the gas behind the SW front.

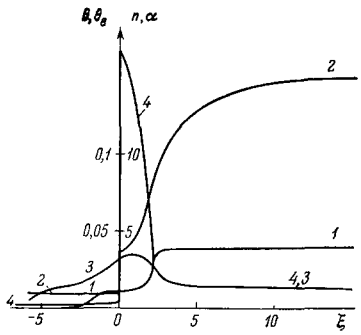

FIG. 21. Structure of a strong SW in air [110], $V_1 \simeq 55$ km/sec, $p_1 \simeq 2.3 \times 10^{-5}$ atm. Curves—plasma parameters: 1—degree of ionization, 2—relative density ρ/ρ_1, 3—relative temperature of the electrons $\theta_e = T_e/2\epsilon_0$, 4—relative temperature of the heavy particles $\theta = T/2\epsilon_0 (\epsilon_0$ is the initial kinetic energy of the atom); $\xi = x/L_i$—reduced distance in units of L_i of the characteristic ionization length corresponding to an equilibrium state behind the front.

concentration and for the temperatures of the ions and electrons. The rate constant for multiple ionization in[110] corresponds to the approximation of immediate ionization. The profiles of the plasma parameters for a typical case are given in Fig. 21. The maximum of T_e in the region behind the jump is due to intense electron heating in elastic collisions with ions (see also Sec. 4.1). The question of the structure of the strong compression jump which was considered infinitely thin in[110] would be interesting under these conditions.

Zheleznyak[90] considered the relaxation behind a SW in nitrogen at velocities of 18—24 km/sec where double ionization is important. The equations for the concentrations of singly and doubly ionized ions were integrated independently. It is obvious (and it is confirmed by the results of[90]) that by virtue of considerations, analogous to those presented in 4.3, the relaxation time of doubly ionized ions should have a nonmonotonic dependence on the velocity.

5. RADIATION OF THE RELAXATION ZONE

The processing of experimental data on the radiation profiles in the relaxation zone can yield more detailed information about the processes occurring in it. In addition, in some cases the radiation of the nonequilibrium zone is of independent interest. The radiation of the nonequilibrium zone attracted special attention after a bright maximum of its intensity was observed behind a SW in air.

5.1. Distribution of Atoms Over the Excited States in a Non-equilibrium Plasma

The concentration of atoms on the k-th state n_k can be calculated by solving a system of balance equations written with respect to each excited state. Collisions between excited atoms can be neglected. The system of equations is therefore linear and can be solved. In the quasistationary approximation (see Sec. 2.1) the solution can be written in the form

$$y_k = r_{1k} y_1 + r_{ke} y_e^2, \qquad (5.1)$$

$y_k = n_k/n_k^0$, $y_e = n_e/n_e^0$. The superscripts "zero" mark quantities corresponding to equilibrium at local values of T_e.

The coefficients r_{1k} and r_{ke} depend on the probabilities of the elementary processes. In addition r_{1k} and r_{ke} depend on T_e and often on the concentration of electrons and on the linear dimensions of the problem. The latter occurs if the emission of reabsorbed radiation affects the populations of the levels. The coefficients r_{1ke} and r_{ke} can be obtained numerically, and tabulated. This was done for certain cases by Bates and his coworkers.[91-93]

Diffusion considerations (see Sec. 2.1) developed for a discrete energy space allow one to obtain analytic expressions for r_{1k} and r_{ke}. Electron-atom, atom-atom collisions, radiative processes and the non-Maxwellian nature of the electron energy distribution are taken into account.[11,13-94] If the kinetics is only determined by collisions with electrons, then r_{1k} and r_{ke} depend only on T_e and are

$$r_{1k} = \sum_{i \geqslant k} S_i / \sum_{i \geqslant 1} S_i, \quad r_{ke} + r_{1k} = 1, \quad S_i = K_i / \langle z_{i,i+1} \rangle, \qquad (5.2)$$

K_i is the ionization equilibrium constant for the i-th state—$A_i \rightleftarrows A^+ + e$. $\langle z_{i,i+1} \rangle$ is the effective probability of excitation. Sufficiently universal formulas have been obtained for $\langle z_{i,i+1} \rangle$:

$$\langle z_{12} \rangle = n_e \Gamma F_1 \Lambda_1 \frac{\mathrm{Ry}^{3/2}}{\sqrt{T_e}(E_1 - E_2)} e^{(E_2 - E_1)/T_e} = n_e \beta_1, \qquad (5.3)$$

$$\langle z_{i,i+1} \rangle = n_e \Gamma \frac{E_{i-1} \Lambda_i \mathrm{Ry}^{3/2}}{(E_i - E_{i-1})(E_{i-1} - E_{i+1})\sqrt{T_e}} e^{-(E_i - E_{i-1})/T_e}, \quad i \geqslant 2; \qquad (5.4)$$

F_1 is given by (2.4) and Λ_i—by the graph in Fig. 1. In using (5.3) and (5.4) close-lying atomic levels must be combined and a total statistical weight must be assigned to them.

For a qualitative analysis it is convenient to use an approximate formula obtained by neglecting discreteness[94]

$$y(E) = y_1 \chi(E/T_e) + y_e^2 [\chi(E_1/T_e) - \chi(E/T_e)]. \qquad (5.5)$$

The function $\chi(x)$ has been introduced in Sec. 2.1. As follows from (5.1) and (5.5), strongly excited states are in relative equilibrium with the electrons $[y(E) \cong y_e^2]$, and low-lying levels are rather close to equilibrium with the ground state $[y(E) = y_1^2]$.

The results of a calculation of the populations of excited atoms carried out in[11-13,94] are in good agree-

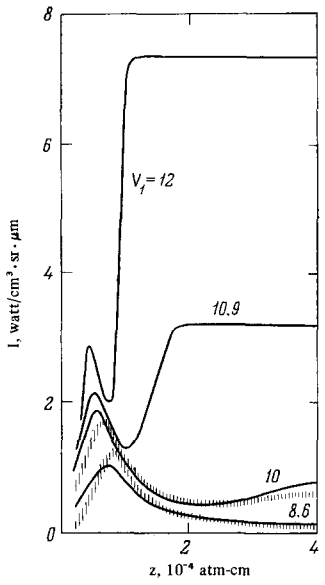

FIG. 22. Profiles of the calculated intensity of the radiation $I_\lambda(z)$ for various velocities of the SW, λ = 0.55–1 μm, $z = p_1 x$. The shading shows the course of oscillograms from [98], p_1 = 0.1 mm Hg.

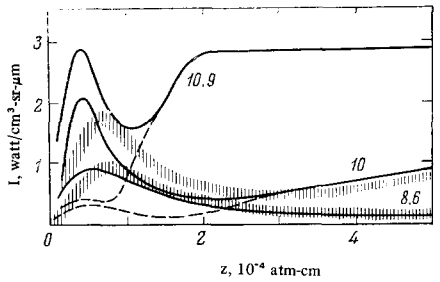

FIG. 23. Comparison of the calculated and experimental (shading) radiation intensity $I_\lambda(z)$ for various SW velocities, λ = 0.40–0.42 μm, $z = p_1 x$, p = 0.1 mm Hg. Dashed curves–contribution of spectral lines.

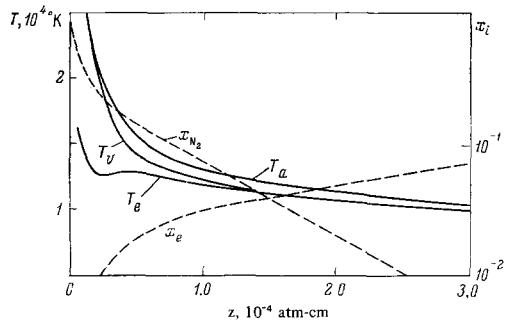

FIG. 24. Profile of parameters behind a SW in air, V_1 = 10 km/sec, p_1 = 0.1 mm Hg, $z = p_1 x$. T_a, T_e, T_v–temperature of the atoms, electrons and vibrations of N_2; x_e and x_{N_2}–molar fractions of electrons and N_2.

ment with experimental data obtained for a broad range of parameters.

5.2. Nonequilibrium Radiation in Spectral Lines and in the Continuum. The Maximum of the Nonequilibrium Radiation

The intensity of the continuum radiation can be calculated in accordance with well-known formulas.[95] It is usually proportional to the square of the concentration of charged particles and increases gradually as one moves away from the front (see Fig. 19). More interesting is the problem of the emission of spectral lines and systems of bands which can pass through a maximum.

For a nonreabsorbed line (k → i transition) the intensity and population profiles of the emitting state k coincide:

$$I_{ki}(x) = A_{ki} y_k n_k^0.$$

If y_k increases monotonically as one approaches equilibrium, then it is clear that for constantly increasing T_e the intensities $I_{ki}(x)$ increase monotonically. However, if a local overheating of electrons takes place in the relaxation zone (see Fig. 11, case 3), then the emission in the spectral line can go through a maximum. Depending on the conditions behind the SW and the scheme of terms of the atom there are various possibilities.*

In mercury vapor the relaxation takes place under local equilibrium; the populations n_k follow the increasing T_e (see Fig. 13). An analogous situation should apparently also prevail in vapors of alkali metals which have, just like mercury, a relatively uniform density of levels.

In inert gases (as well as in nitrogen and oxygen atoms) $E_1 - E_2$ is large and strongly excited states are close to equilibrium with the electrons ($y_k \sim y_e^2$) and thus "follow" the course of n_e (see, for example, the measurements in[61]). When the relaxation follows scheme 3 of Fig. 11, the populations of low-lying excited states can exceed the equilibrium values; this happens in air.

In Figs. 22 and 23 we present oscillograms of the radiation intensity behind a SW in air in two different spectral ranges. The oscillograms have been borrowed from[98,99]. The problem of the mechanism responsible for the appearance of the maximum has been repeatedly discussed in the literature, for example in[100-102]. The proposed explanations made use of unfounded assumptions and fragmentary information about individual processes and did not describe the entire aggregate of observed phenomena. Satisfactory results could only be obtained with the use of an actual distribution of particles over the excited states and with allowance for the heating of electrons by the vibrations of the molecules (see Sec. 2.3). The reasons for the appearance of the radiation peak behind strong SW and its disappearance with increasing V_1 were explained in[103,104] which are of a rather qualitative nature. In[26] the radiation of the nonequilibrium zone is calculated and compared with experiment in the entire frequency spectrum for various SW velocities. Let us discuss the obtained results.

In Fig. 24 we present the profiles of the main parameters of a nonequilibrium plasma. Unlike in the case of weak SW,[36] behind strong SW the vibrational temperature T_v becomes rapidly quasistationary and approaches T_a. However, as n_e increases the vibrations "cool off" intensively in collisions with electrons and T_v, separating from T_a, approaches T_e. The electron energy balance is shown in Fig. 3. Intensive heating by collisions

*Nonequilibrium radiation has been observed in mixtures of Cr + Ar and Ti + Ar behind reflected SW. [96,97] The radiation in the Cr I, Ti I, and Ti II lines (unlike that of Cr II) goes through a maximum. The model of the ionization kinetics used in [96,97] is rather unsatisfactory and is hardly capable of describing the observed effects.

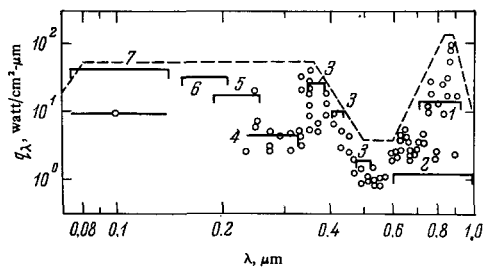

FIG. 25. Spectral radiation fluxes q_λ from the nonequilibrium zone, V_1 = 10 km/sec, p_1 = 0.1 mm Hg. Points–experiment. [98,99] Calculated magnitudes of the flux [26]: 1–3p–3s lines; 2–I positive system of N_2; 3–I negative system of N_2^+; 4–β system of NO; 5–γ system of NO; 6–δ and ε systems of NO; 7–transitions to the ground state of N and O.

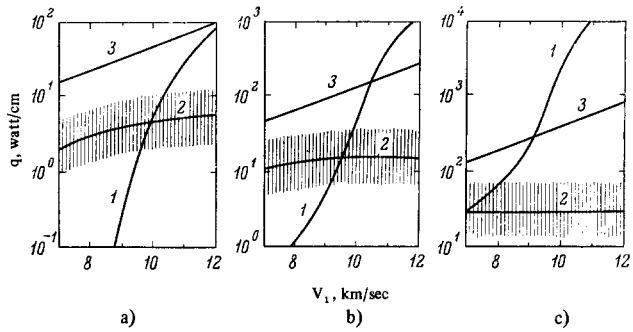

FIG. 26. Thermal flux to a streamlined body as a function of V_1 for various pressures ahead of the front p_1. a) p = 0.01; b) 0.1; c) 1 mm Hg. Radius of bluntness R = 3 m. Curves: 1–radiant flux calculated in the approximation of a compressed equilibrium layer [108]; 2–radiant flux from the nonequilibrium region (shading–proposed uncertainty of the calculation [26]; 3–convective flux. [109]

with vibrationally excited molecules (see Sec. 2.3) led to the circumstance that T_e exceeded appreciably its equilibrium value. This will, in the final analysis, insure a radiation maximum.

Profiles of the calculated radiation intensity for the wavelength range λ = 0.55–1 μm which is determined by the nitrogen and oxygen lines (mainly 3p–3s transitions; the contribution of the continuum and of the bands is small) are presented in Fig. 22 for various SW velocities. The theory is in satisfactory agreement with experiment. The oscillograms of[98,99] were normalized in accordance with the calculated values of the radiation of the equilibrium zone.[106] It follows from Fig. 22 that although with increasing V_1 the intensity in the maximum indeed increases, its ratio to the equilibrium level drops, and the phenomenon of the maximum disappears gradually. This is explained by the more rapid dissociation of N_2 behind the front.

Analogous dependences for the range λ = 0.40–0.42 μm are presented in Fig. 23. The contribution of these or other processes to the spectral intensity I_λ can be different. The first negative system of bands of N_2^+ predominates in the region of the maximum, but on approaching equilibrium there is an increase in the role of the atomic lines (4p – 3s transitions) whose contribution for V_1 = 10 and 10.9 km/sec is given by the dashed curves.

In Fig. 25 we present the spectral radiation fluxes from the nonequilibrium zone under the same conditions. The calculated radiation level of the principal spectral components averaged in the indicated wavelength ranges is shown. The calculation and experiment agree over the entire spectrum.

The radiation maximum in the nonequilibrium zone for low SW velocities is also observed in other molecular gases–nitrogen and mixtures of CO_2 and N_2 (see, for example[65,107]). At present there is no satisfactory theory, a fact which is due to the diversity and complexity of the elementary processes in a molecular plasma.

5.3. The Effect of Processes in the Relaxation Zone on the Aerodynamic Heating in Hypersonic Flow

The investigation of the structure of SW in molecular gases is of interest in connection with the entry problem of space apparatus into the dense layers of the atmosphere. As is well known, a separating SW is produced ahead of a body moving in a gas with hypersonic velocity. The distance between the SW front and the frontal portion of the body surface is ~ 0.05 R where R is the radius of bluntness.

The high temperature and pressure in the compressed layer give rise to large values of the convective heat flux towards the surface of the body. The radiation of the compressed layer may make a considerable contribution to aerodynamic heating.[108] With increasing velocity the radiation fluxes increase sharply and can exceed the convective fluxes appreciably.

A knowledge of the characteristic relaxation times makes it possible to determine the structure of the SW and establish conditions under which the nonequilibrium zone and boundary layer coalesce, a circumstance which determines the limits of applicability of the existing theory of convective heating. An even more important problem is the effect of radiation of the nonequilibrium zone on radiative heating. This problem arose after the observation of an emission maximum in the nonequilibrium layer behind a SW. The effect of this phenomenon on the magnitude of radiative heating has been repeatedly discussed in the literature. Considerable progress was made in[26]. It was shown that at comparatively low velocities, when the maximum of the nonequilibrium radiation is particularly large, radiative heating is as a whole small compared with convective heating. At higher velocities, when the relationship between the radiative and convective components of aerodynamic heating becomes inverse, radiative heating is almost completely determined by radiation from the equilibrium zone (Fig. 26).

Thus the contribution of nonequilibrium radiation to aerodynamic heating need not be taken into account. This result was obtained for motion in the atmosphere of the earth and may be different for other planets.

[1] Ya. B. Zel'dovich and Yu. P. Raĭzer, Usp. Fiz. Nauk 63, 613 (1957).

[2] Ya. B. Zel'dovich and Yu. P. Raĭzer, Fizika udarnykh voln i vysokotemperaturnykh gazodinamicheskikh yavleniĭ (The Physics of Shock Waves and High-temperature Gasdynamic Phenomena), Nauka, 1966.

[3] S. A. Losev and A. I. Osipov, Usp. Fiz. Nauk 74, 393 (1961) [Sov. Phys.-Uspekhi 4, 525 (1962)].

[4] E. V. Stupochenko, S. A. Losev, and A. I. Osipov,

Relaksatsionnye protsessy v udarnykh volnakh (Relaxation Processes in Shock Waves), Nauka, M. 1966.

[5] J. W. Bond, K. M. Watson, and J. A. Welch, Atomic Theory of Gas Dynamics, Addison-Wesley, 1965 (Russ. Transl., Mir, M. 1968).

[6] E. Bauer, JQSRT 9, 499 (1969).

[7] K. Schofield, Planet. Space Sci. 15, 643 (1967).

[8] F. R. Gilmore, E. Bauer, and J. W. McGowan, JQSRT 9, 157 (1969).

[9] H. E. Petschek and S. Byron, Ann. Phys. 1, 270 (1957).

[10] S. T. Belyaev and G. I. Budker, Coll. Fizika plazmy i problema upravlyaemykh termoyadernykh reaktsiĭ (Plasma Physics and the Problem of Controllable Thermonuclear Reactions) v. 3, AN SSSR, M. 1958, p. 41.

[11] L. M. Biberman, V. S. Vorob'ev, and I. T. Yakubov, Teplofizika vysokikh temperatur 5, 201 (1967); 6, 369 (1968); 7, 593 (1969).

[12] L. M. Biberman, V. S. Vorob'ev, and I. T. Yakubov, Coll. Magnitogidrodinamicheskiĭ metod polucheniya elektroenergiĭ (Magnetohydrodynamic Method of Obtaining Electrical Energy), Énergiya, M. 1968, p. 209.

[13] L. M. Biberman, V. S. Vorob'ev, and I. T. Yakubov, Zh. Eksp. Teor. Fiz. 56, 1992 (1969) [Sov. Phys.-JETP 29, 1070 (1969)].

[14] D. R. Bates, A. E. Kingston, and R. W. P. McWhirter, Proc. Roy. Soc. A276, 297 (1962); A270, 152 (1962).

[15] L. P. Pitaevskii, Zh. Eksp. Teor. Fiz. 42, 1326 (1962) [Sov. Phys.-JETP 15, 919 (1962)]; A. V. Gurevich and L. P. Pitaevskii, Zh. Eksp. Teor. Fiz. 46, 281 (1964) [Sov. Phys.-JETP 19, 870 (1964)].

[16] N. M. Kuznetsov and Yu. P. Raĭzer, PMTF No. 4, 10 (1965).

[17] V. A. Abramov and B. M. Smirnov, Optika i spektroskopiya 21, 19 (1966).

[18] L. M. Biberman, V. S. Vorob'ev, A. N. Lagar'kov et al., Izv. AN SSSR, Mekh. Zhidkost. Gaz. No. 6, 46 (1967).

[19] M. B. Zheleznyak and A. Kh. Mnatsakanyan, Teplofizika vysokikh temperatur 6, 390 (1968).

[20] L. M. Biberman, V. S. Vorob'ev, and I. T. Yakubov, Teplofizika vysokikh temperatur 7, 193 (1969).

[21] J. B. Hasted, Physics of Atomic Collisions, Butterworths, 1964 (Russ. Transl., Mir, M. 1965).

[22] B. M. Smirnov, Atomnye stolknoveniya i elementarnye protsessy v plazme (Atomic Collisions and Elementary Processes in a Plasma), Atomizdat, M. 1968.

[23] M. N. Mentzoni and R. V. Row, Phys. Rev. 130, 2312 (1963).

[24] G. J. Schulz, Phys. Rev. 116, 1141 (1959); 125, 229 (1962); 135A, 988 (1964).

[25] L. M. Biberman and A. Kh. Mnatsakanyan, Report N SM-74/215 in Electricity from MHD, v. 2, Vienna 1966, p. 107; Teplofizika vysokikh temperatur 4, 491 (1966).

[26] M. B. Zheleznyak, A. Kh. Mnatsakanyan, and I. T. Yakubov, Izv. AN SSSR, Mekh. Zhidkost. Gaz. No. 4, 161 (1970).

[27] V. A. Kas'yanov and L. I. Podlubnyĭ, Coll. Doklady yubileĭnoĭ nauchno-tekhnicheskoĭ konferentsii MÉI, Fizika (Trans. of the Anniversary Scientific-technical Conference of the Moscow Power Institute, Physics), Énergiya, M. 1967, p. 131.

[28] R. S. Amme and P. O. Haugsiaa, Phys. Rev. 177, 230 (1969).

[29] J. W. Bond, Phys. Rev. 105, 1683 (1957).

[30] H. D. Weymann, Bull. Amer. Phys. Soc. 4, 284 (1959).

[31] K. E. Harwell and R. G. Jahn, Phys. Fluids 7, 214 (1964).

[32] A. J. Kelly, J. Chem. Phys. 45, 1723, 1733 (1966).

[33] J. T. McLaren and R. M. Hobson, Phys. Fluids 11, 2162 (1968).

[34] P. E. Oettinger and D. Berchader, AIAA J. 5, N9 (1967).

[35] D. J. Hollenbach and E. E. Salpeter, J. Chem. Phys. 50, 4157 (1969).

[36] S. C. Lin and J. D. Tear, Phys. Fluids 6, 355 (1963).

[37] W. H. Kasner, Phys. Rev. 164, 194 (1967).

[38] L. Frommhold and M. A. Biondi, Bill. Amer. Phys. Soc. 12, 217 (1967).

[39] F. J. Mehr and M. A. Biondi, Phys. Rev. 181, 264 (1969).

[40] J. Wilson, Phys. Fluids 9, 1913 (1966).

[41] G. D. Smekhov, Dissertation, Scientific Research Institute of Mechanics of the Moscow State University, 1968; S. A. Losev and G. D. Smekhov, Teplofizika vysokikh temperatur 7, 1015 (1969).

[42] T. R. Connor and M. A. Biondi, Phys. Rev. 140, A778 (1965).

[43] C. F. Hansen, Phys. Fluids 11, 904 (1968).

[44] I. S. Gulledge, D. M. Packer, S. Tilford, and G. Wilkinson, J. Geophys. Res. 73, 5535 (1968).

[45] L. M. Biberman, Zh. Eksp. Teor. Fiz. 17, 416 (1947).

[46] L. M. Biberman, Dokl. Akad. Nauk SSSR 49, 659 (1948); Nizkotemperaturnaya plazma, Trudy 20 Kongressa YuPAK (Low-temperature Plasma, Trans. Twentieth Congress of IUPAC), Mir, M. 1968, p. 931.

[47] A. N. Lagar'kov, Teplofizika vysokikh temperatur 4, 305 (1966); E. I. Asinovskiĭ, E. V. Drokhanova, A. V. Kirillin, and A. N. Lagar'kov, Teplofizika vysokikh temperatur 5, 747 (1967).

[48] L. M. Biberman and B. A. Veklenko, Zh. Eksp. Teor. Fiz. 37, 164 (1959) [Sov. Phys.-JETP 10, 117 (1960)].

[49] A. N. Lagar'kov and I. T. Yakubov, Optika i spektroskopiya 14, 199 (1963).

[50] K. A. Alpher and D. R. White, Phys. Fluids 2, 162 (1959).

[51] S. S. R. Murthy, JQSRT 8, 531 (1968).

[52] L. M. Biberman and I. T. Yakubov, Zh. Tekh. Fiz. 33, 1344 (1963) [Sov. Phys.-Tech. Phys. 8, 1001 (1964)].

[53] N. M. Kuznetsov, Zh. Tekh. Fiz. 34, 625 (1964) [Sov. Phys.-Tech. Phys. 9, 483 (1964)].

[54] J. H. Clarke and C. Ferrari, Phys. Fluids 8, 2121 (1965).

[55] H. F. Nelson, Purdue University Report No. AAEES 67-9 (1968).

[56] G. M. Lawrence, Phys. Rev. 175, 40 (1968).

[57] R. S. Knox, Phys. Rev. 110, 375 (1958); A. Gold and R. S. Knox, Phys. Rev. 113, 834 (1959).

[58] G. K. Tumakaev and V. R. Lazovskaya, Coll. Aerofizicheskie issledovaniya sverkhzvukovykh techeniĭ (Aerophysical Investigations of Supersonic Flow), Nauka, 1967, p. 74.

[59] J. Smith, Phys. Fluids 11, 2150 (1968).
[60] T. V. Zhikhareva and G. K. Tumakaev, Teplofizika vysokikh temperatur 8, 40 (1970).
[61] G. I. Kozlov, Yu. P. Raĭzer, and D. I. Roĭtenburg, PMTF No. 1, 140 (1968).
[62] S. A. Losev, G. D. Smekhov, and V. A. Polanskiĭ, Khimiya vysokikh énergiĭ 2, 478 (1968).
[63] J. W. Bond, Coll. Na poroge v kosmos (At the Threshold of the Cosmos) IL, M. 1960, p. 343.
[64] D. L. Chubb, Phys. Fluids 11, 2363 (1968).
[65] R. A. Allen, JQSRT 5, 511 (1965).
[66] A. Kh. Mnatsakanyan and L. I. Podlubnyĭ, Teplofizika vysokikh temperatur 8, 33 (1970).
[67] M. I. Hoffert and H. Lien, Phys. Fluids 10, 1769 (1967).
[68] Yu. S. Lobastov and V. G. Testov, Teplofizika vysokikh temperatur 7, 358 (1969).
[69] E. J. Morgan and R. D. Morrison, Phys. Fluids 8, 1608 (1965).
[70] B. H. Wong and D. Bershader, J. Fluid Mech. 26, 459 (1966).
[71] N. R. Jones and M. McChesney, Nature 209, 1080 (1966).
[72] P. Gloersen, J. Chem. Phys. 28, 820 (1958).
[73] W. Roth, J. Chem. Phys. 31, 844 (1959).
[74] P. Gloersen, Phys. Fluids 3, 857 (1960).
[75] J. A. Smith, Phys. Fluids 11, 2150 (1968).
[76] H. S. Johnston and W. Kornegay, Trans. Farad. Soc. 57, 1563 (1961); J. Chem. Phys. 38, No. 9 (1963).
[77] G. K. Tumakaev and V. R. Lazovskaya, Zh. Tekh. Fiz. 34, 1879 (1964) [Sov. Phys.-Tech. Phys. 9, 1449 (1965)].
[78] R. M. Hill and B. Capp, Nature 208, 176 (1965).
[79] A. F. Hought, Phys. Fluids 5, 1337 (1963).
[80] I. T. Yakubov, Zh. Tekh. Fiz. 34, 879 (1964) [Sov. Phys.-Tech. Phys. 9, 676 (1964)].
[81] W. Lindemann, J. Czech. Physikal. Institut der Technischen Hochschule, Aachen, Bericht HMR 124, 1969.
[82] L. M. Biberman and I. T. Yakubov, Teplofizika vysokikh temperatur 3, 340 (1965).
[83] S. C. Lin, R. A. Neale, and W. I. Fyfe, Phys. Fluids 5, 1633 (1963).
[84] R. A. Allen, A. Textoris, and J. Wilson, JQSRT 5, 95 (1965).
[85] S. A. Losev and V. A. Polanskiĭ, Izv. Akad. Nauk SSSR, Mekh. Zhidkost. Gaz. No. 1, 176 (1968).
[86] R. Gulard, R. E. Bugner, R. K. Berns, and G. F. Nelson, Teplofizika vysokikh temperatur 7, 542 (1969).
[87] J. H. Clarke and M. Onorato, Division of Engineering, Brown University, Providence, Report Nonr-562 (35)/22 (1969).
[88] C. A. Whitney and A. J. Skalafuris, Ap. J. 138, 200 (1963).
[89] I. T. Yakubov, Optika i spektroskopiya 19, 26 (1965).
[90] M. B. Zheleznyak, PMTF No. 6 (1970).
[91] D. R. Bates, A. E. Kingston, and R. W. McWhirter, Proc. Roy. Soc. A270, 155 (1962).
[92] D. R. Bates and A. E. Kingston, Planetary and Space Sci. 2, 1 (1963).
[93] D. R. Bates and A. E. Kingston, Proc. Phys. Soc. 83, 43 (1964).
[94] V. S. Vorob'ev, Zh. Eksp. Teor. Fiz. 51, 327 (1966) [Sov. Phys.-JETP 24, 218 (1967)].
[95] L. M. Biberman and G. É. Norman, Usp. Fiz. Nauk 91, 193 (1967) [Sov. Phys.-Uspekhi 10, 52 (1967)].
[96] W. L. Shakelford and S. S. Penner, J. Chem. Phys. 45, 1816 (1966).
[97] A. A. Boni, Jr., J. Chem. Phys. 49, 3885 (1968).
[98] R. A. Allen, P. H. Rose, and J. C. Camm, IAS Paper No. 63-77 (1963).
[99] R. A. Allen, R. L. Taylor, and A. Textoris, Proc. VI Conf. International Phenom. d'Ionis. dans les gas, Paris, v. 3, 1963, p. 381.
[100] J. D. Tear, S. Georgiev, and R. A. Allen, Hypersonic Flow Research, (F. R. Riddel, ed.), Academic Press, N. Y. 1962, p. 281. Transl. in Coll. Issledovanie sverkhzvukovykh techeniĭ (Investigation of Supersonic Flow), Mir, M. 1964.
[101] A. K. Artamonov, V. N. Arkhipov, and G. E. Starchenko, Izv. Akad. Nauk SSSR, Mekh. Zhidkost. Gaz. No. 3, 20 (1966).
[102] A. D. Nadezhin and E. A. Romishevskiĭ, PMTF No. 1, 27 (1969).
[103] I. T. Yakubov, Teplofizika vysokikh temperatur 5, 515 (1967).
[104] V. S. Vorob'ev and I. T. Yakubov, ZhETF Pis. Red. 4, 43 (1966) [JETP Lett. 4, 28 (1966)].
[105] V. A. Bronshten, Problemy dvizheniya v atmosfere krupnykh meteoritnykh tel (Problems of Motion of Large Meteoritic Bodies in the Atmosphere), AN SSSR, M. 1963.
[106] I. V. Avilova, L. M. Biberman, V. S. Vorob'ev, et al. JQSRT 9, 89, 113 (1969).
[107] F. Wolf and J. Spiegel, J. Spacecraft and Rockets 4, 1166 (1967).
[108] L. M. Biberman, V. S. Vorob'ev, G. E. Norman, and I. T. Yakubov, Kosmicheskie issledovaniya 2, 441 (1964).
[109] J. A. Fay and F. R. Riddel, J. Aerospace Sci. 25, 73 (1958).
[110] N. N. Magretova, M. G. Pashchenko, and Yu. P. Raĭzer, PMTF No. 6 (1970).

Note added in proof. We shall indicate papers which became known to us after the submission of the manuscript to the editor. Precursor concentrations of electrons ahead of the SW were measured in [1,2] for argon and in [3] for air. The ionization kinetics behind the SW front was investigated for xenon in [4], for argon in [5], and for hydrogen in [6]

[1] H. D. Weymann, Phys. Fluids 12, 1193 (1969).
[2] L. B. Holmes and H. D. Weymann, Phys. Fluids 12, 1200 (1969).
[3] M. Omura and L. L. Presley, AIAA J. 7, No. 12, 2363 (1969).
[4] N. A. Generalov, V. P. Zimakov, and G. I. Kozlov, Zh. Eksp. Teor. Fiz. 58, 1928 (1970) [Sov. Phys.-JETP 31, 1038 (1970)].
[5] G. D. Smekhov and Yu. S. Lobastov, Zh. Tekh. Fiz. 40, 1660 (1970) [Sov. Phys.-Tech. Phys., No. 8 (1971)].
[6] Y. Nakagawa and D. C. Wisler, Book of Abstracts Seventh International Shock Tube Symposium, Institute of Aerospace Studies, University of Toronto, Toronto, 1969, p. 124.

Translated by Z. Barnea